

Original scientific paper

UDC 556.166:[502.211:582](65)
<https://doi.org/10.2298/GSGD2401073B>

Received: October 09, 2023

Corrected: November 01, 2023

Accepted: November 29, 2023

Ali Berghout^{1*}, Mohamed Meddi^{2}**

** Laboratory of Water, Environment and Renewable Energies. Faculty of Technology. University of M'sila, PO Box 160 Ichebilia, 28000 M'sila, Algeria*

*** Higher National School of Hydraulics – BLIDA, Algeria*

EFFECTS OF SEASONAL CHANGES IN VEGETATION COVER ON THE HYDROLOGICAL RESPONSES OF THE CHEMORA WADI CATCHMENT TO EXTREME RAINFALL

Abstract: The choice of the reference flood for the dimensioning of hydraulic structures is rather delicate, in particular in the not gauged basins. In these basins, the estimation of the project flood requires the use of predetermined methods based on the maximum daily precipitation. In this context, this work consists of evaluating the impact of seasonal changes in vegetation cover on the hydrological responses of the watershed to extreme precipitation events in terms of peaks and water volumes using the HEC-HMS model. The study was based on rainfall and discharge data recorded at rainfall and hydrometric stations in the Wadi Chemora basin (Algeria), in addition to remote sensing data on a monthly scale. The results show that the estimation of the projected flood using methods based only on maximum daily rainfall in semi-arid areas is insufficient, which shows the interest of considering the effects of these changes.

Key words: curve number, extreme floods, HEC-HMS, NDVI, Wadi Chemora watershed, rain-flow.

¹ ali.berghout@univ-msila.dz (corresponding author)

Ali Berghout (<https://orcid.org/0000-0002-7436-7927>)

Mohamed Meddi (<https://orcid.org/0000-0002-9772-7366>)

Introduction

Time series flows are necessary for water resources management and the sizing of hydro-technical infrastructures as well as for watershed management, however most of the watersheds are not gauged or are only poorly gauged, which leads to the existence of insufficient information. Many approaches have been developed and used worldwide to answer this question. These include regionalization for transferring hydrological information from gauged to ungauged catchments (Sarhadi & Modarres, 2011; Johnson et al., 2012; Razavi & Coulibaly, 2012; Meddi et al., 2017), as well as the ensemble modeling approach and the combination of several models (Velázquez et al., 2010; Li & Sankarasubramanian, 2012; Abdi & Meddi, 2020a; Abdi & Meddi, 2020b).

The vegetation cover plays an important role in the transformation of rain into a flow and consequently on flooding in a given area (Arshad et al., 2020). Studying the influence of vegetation on hydraulic hazards is therefore of great importance for planning and decision-making in the management of said hazards and the dimensioning of protective structures (Benifei et al., 2015; Apollonio et al., 2016; Shrestha, 2019; Yahi & Rezoug, 2019). A vegetation cover in good condition creates a mask on the surface of the soil, thus blocking the path of water trickles and increasing water infiltration (Cerdà, 1998) it also reduces runoff in terms of peaks and volumes (Combes et al., 1995; Lavabre & Andreassian, 2000). Moreover, it increases the minimum rainfall threshold to obtain runoff, and which then causes a reduction in the frequency of floods (Richard & Mathys, 1999). However, according to McIvor et al. (1995), it weakens daily rain with more than 100 mm and an intensity greater than 45 mm h⁻¹ and the runoff and peak flow in impermeable surfaces are greater and the concentration-time is shorter (Vasiliki et al., 2020).

The study aims to evaluate the effects of the vegetation cover's seasonal changes on the hydrological responses of draining basins located in semi-arid zones of extreme precipitation in terms of peaks and water volumes. The study consists of hydrological modeling by the HEC-HMS code under the SIG, which aims to understand the formation of floods and assess the impact of vegetation on flooding. This approach was widely used to predict flows taking into account land use and vegetation cover (Mendas et al., 2008; Ibrahim-Bathis & Ahmed, 2016; Scharffenberg, 2016; Koneti et al., 2018; Zheng et al. 2020; Hu & Shrestha, 2020).

The first part of this study will involve the calibration and validation of the HEC HMS model using data of the floods and the vegetation cover of the wadi Chemora basin in the east of Algeria. The second component will assess the effect of seasonal variation in vegetation cover conditions on the production of Chemora wadi flows from extreme. The HEC-HMS hydrological model has several advantages, notably liquid flows estimate, sediment loads in rivers, average speed through cross-sections and water line by exploiting data from precipitation and using possible combinations of different calculation methods of model settings (Scharffenberg, 2016).

In this view, the study aims at evaluating the effects of the vegetation cover's seasonal changes on the hydrological responses of draining basins located in semi-arid zones of extreme precipitation in terms of peaks and water volumes. The assessment of maximum flows is necessary to protect the city from flooding by building new structures based on these predictions.

Material and Methods

Study area

The Chemora watershed is located on the northern foothills of Aurès (Batna Algeria), circumscribed in the great basin of High Plateaux of Constantine numbered 07 according to the nomenclature adopted by the National Hydric Resources Agency (NHRA) (Figure 1) (NHRA 2005). It covers an area of 763.4 km². The upstream part of the basin consists of three sub-basins namely (Berghout & Meddi 2016):

1. Basin Oued Rbôa in the East with an area of 297.9 km², equipped with a hydrometric station downstream (site Rbôe).
2. Oued Soudhes Basin to the West occupying an area of 192.9 km², equipped with a hydrometric station downstream (Timgad site).
3. Oued Morri Basin occupying the center of the basin with an area of 21.9 km², equipped with a hydrometric station downstream (Morri site).

The confluence of the wadis draining these sub-basins from Oued Chemora is lost after a journey of about 30 km, in the salt lakes of the high Constantine plains. It is equipped with a hydrometric station located upstream of the city of Chemora.

The overflowing of the Chemora wadi is causing huge problems linked to the repeated flooding recorded in the town of Chemorah. The floods of August 2017 caused extensive damage to homes, administrations and roads. On 30 October 2011, heavy rain raised the level of the Wadi Chemora, causing dozens of residents to become isolated. Heavy rainfall in May 2021 caused massive flooding, damaging roads and flooding many homes (rainfall in some places exceeded 70 mm in 24 hours). This situation demonstrates the city's vulnerability to repeated flooding in recent years, despite the construction of a dam with a capacity of 65 million m³ upstream (around 30 km) and the construction of a canal in the centre of the city. Changes in the vegetation cover in the catchment area have led to an increase in the flows that cause flooding.

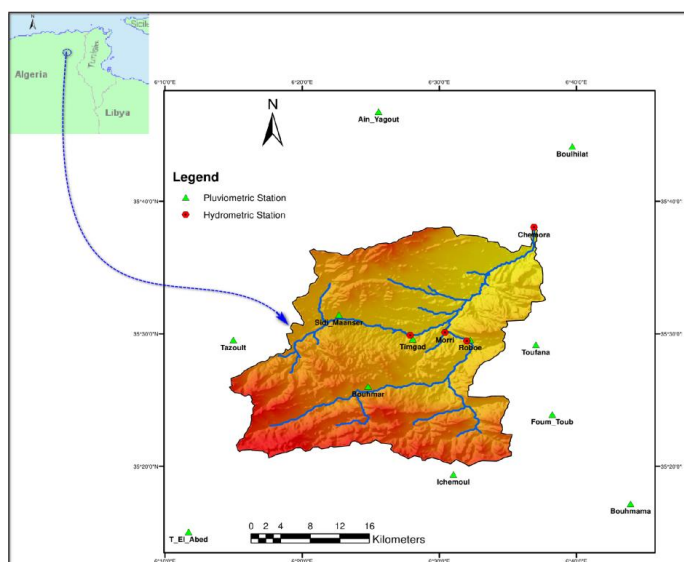


Fig. 1. Wadi Chemora Watershed

This study will be based on rainfall recorded at the twelve rainfall stations located in and around the Oued Chemora basin (Thniet El-Abed, Ichemoul, Tazoult, Bouhmar, Reboe, Timgad, Sidi Maansar, Boulhilat, Bouhmama, Toufana, Ain Yagout, and Foug Toub) (Figure 1), the water levels measured at the 4 hydrometric stations controlling the basin (Reboe, Morri, Timgad, and Chemora) (Figure 1) as well as LANDSAT5 satellite images and soil data from soilgrids.org.

Methodology

The HEC-HMS software takes into account precipitation (Weather Module), losses by infiltration and evapotranspiration (Module of the production function), direct runoff that takes into account surface flows, storages and pressure drops (transfer function module), and the behavior of the water when it is in the river bed (routing module) (USAID, 2013).

The combination chosen to model these different parameters is dictated mainly by the available data as follows:

- The adopted weather module is the Natural Resources Conservation Service (NRCS), which has overcome the problem of missing pluviograph data (USACE, 2013).
- The NRCS CN (curve number) method chosen for the production function is simple, faithful, does not require huge amounts of data, and directly depends on a single parameter that contains three basic factors in the rainfall-flow modeling (land use, soils, and antecedent moisture), according to the following equation (USACE, 2013):

$$Pe = \frac{(P - Ia)^2}{P - Ia + S} \quad (1)$$

where:

Pe is the net precipitation at time t;

P is the the gross precipitation at time t; Ia is the initial abstraction; S is the maximum retention potential.

The NRCS has proposed an additional empirical relationship linking the initial abstraction of a watershed to the maximum retention potential (USACE, 2013):

$$Ia = 0.2 \times S \quad (2)$$

The influence of the first two factors mentioned above is estimated by the parameter CN which is connected to S by the equation (USACE, 2013):

$$S = \frac{25400 - 254CN}{CN} \quad (3)$$

The selected transfer function is the unit hydrograph of the NRCS, this function does not require a lot of data, and show satisfactory results (Chang, 2009). This function expresses the rate Ut as proportional to the peak flow rate Up, for each time t, fraction of the peak time Tp (USACE, 2013).

$$Up = C \frac{A}{Tp} \quad (4)$$

where:

A is the surface of the watershed and C is the conversion constant (2.08 for the international system).

The peak time Tp is related to the duration of the net rainfall by the formula:

$$Tp = Tlag \frac{\Delta t}{2} \quad (5)$$

where:

Δt is the duration of the net rain (this is the step of simulation time);

$Tlag$ is the Lag in hours of the basin (difference between the peak of the net rainfall and the peak of the hydrograph), where the $Tlag$ is calculated by the NRCS formula defined as follows:

$$Tlag = L^{0.8} \times \left(\left(\left(\frac{1000}{CN} \right) - 1 \right) + 1 \right)^{0.7} \frac{1}{1900 \sqrt{Y}} \quad (6)$$

where:

L is the length from the outlet to the upstream of the largest stream in the foot; CN is the composite curve number of the basin; Y is the basin slope in %.

The routing function chosen is that of the Lag, this function also simple, do not require a lot of data. This function assumes that the output hydrograph is simply the hydrograph of the entered flow, of a specified duration, which is the time taken by the flood in the stream bed.

According to Kirpich's method, this time is given by the following equation (USDA, 2010):

$$Lag = Tch = K L k^{0.77} S^{-0.385} \quad (7)$$

where:

Lag = Tch is the Time taken by the flood in the stream in min;

K = 0.0078 for the international system;

L is the length of watercourse (m);

S is the slope of the water course (m / m).

The shape of the base flow chosen is the exponential recession; it is best suited to the semi-arid context.

$$Qt = Q0 x k^t \quad (8)$$

where:

Qt is the flow at time t;

Q0 is the initial flow;

K is the exponential decay constant

Data Preparation

In this model, the watershed has been divided into nine sub-basins to have units that are more or less homogeneous from a lithological and hydrological point of view. The latter is drained by a hydrographic network formed by nine talwegs (Figure 2). In order to evaluate the factors necessary for the combination of the chosen modeling and by using the ASTER satellite images, we have been able to trace slope maps, we have used data from soilgrids.org in order to trace land map types NRCS and waterproof percentage map.

a- The map slopes: The Digital Terrain Model (DTM) used in this study comes from ASTER images. This DEM, with a resolution of 30 x 30 m is sufficient for this study (Nazari-Sharabian et al., 2020). This model was used for the extraction of various physiographic parameters of the watershed including the slope (Figure 3).

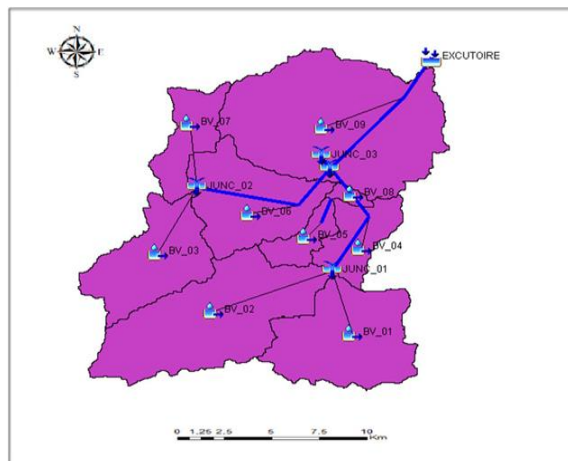


Fig. 2. Cutting of the Chemora Watershed

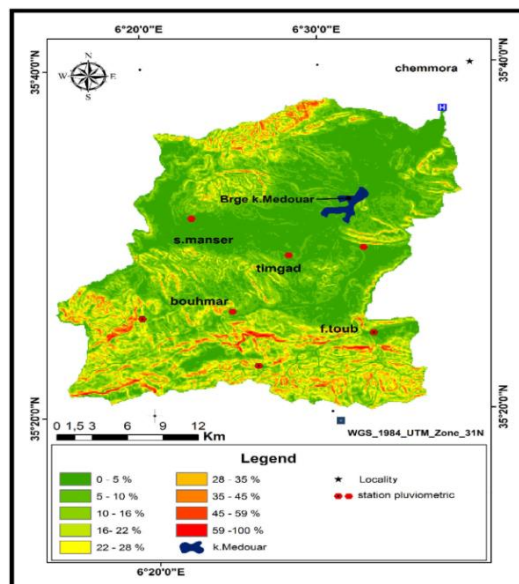


Fig. 3. Chemora Watershed Slope Map

b- NRCS floor card: The NRCS Soil Map (Figure 4) is developed using soil data available at <https://soilgrids.org/> following the NRCS classification, which defines land cover classes into four major groups (Cane, 1985):

- Group "A": soils with low runoff potential.
- Group "B": soils with a moderate rate of infiltration and medium transmissivity.
- Group "C": soils with slow infiltration rate and low transmissivity.
- Group "D": soils with high runoff potential.

c- The map of the percentage of raincoats: The percentage of impervious designates the portion of the surface of the pond considered as watertight and directly connected to the drainage network. The map of the percentage of impervious (Figure 5) was developed using the data available at the site: <https://soilgrids.org/>.

d- NDVI and CN maps: In this study, we used the NDVI derived standardized vegetation index approach in order to calculate the CN. This approach was determined by LANDSAT5 satellite images from September 1990 to August 1991 and from September 1995 to August 1996 adapted to the NRCS classification.

This approach has been used to obtain approximate values for the CN factor the value of CN depends on the nature of the vegetation, percentage of vegetation cover, and land use. To estimate the values of CN from that of the NDVI, we divided the latter into 7 classes (Table 1 and Figure 6):

Very dense vegetation: Represented by cedar forests (pure or mixed with other species such as evergreen oak and oxycedar, etc.).

Dense vegetation: This class is represented by oak forests, holm oak (*Quercus ilex*), and cork oak (*Quercus suber*), with the presence of pine forests generally Aleppo pines (*Pinus halepensis*).

Degraded vegetation: Generally, matorrals characterized by the dominance of shrubs with evergreen leaves, large and small, rigid, and thick, with small trees sometimes present with or without undergrowth.

Very degraded vegetation Generally degraded and scrubland maquis that contains an association of plants rarely exceeding the shrub stage.

Sparse vegetation: Degraded scrubland where the shrub vegetation is less dense and the tree layer is absent, scattered throughout the area, these scrublands are dominated essentially by the wild jujube (*Ziziphus lotus*), the asphodel (*Asphodelus Microcarpus*), the dwarf palm (*Chamaerops Humilis*) ... etc.

Bare Soils: This class includes the bare soils of therophyte formations (Emes).

The surface of water bodies: Includes the surface of the Kodiet Meddaouer dam water body and the surfaces of watercourses.

e-The rainfall maps: The precipitation maps corresponding to events recorded during the periods mentioned above were plotted from the rainfall recorded 12 rainfall stations located in and in the vicinity of the watershed (Figure 7) (NHRA, 2005).

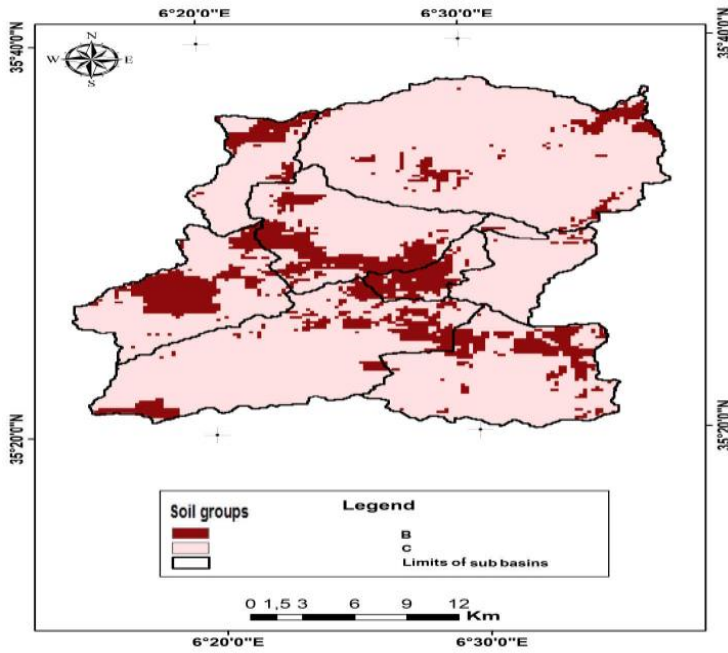


Fig. 4. NRCS Soil Map of the Chemora Watershed

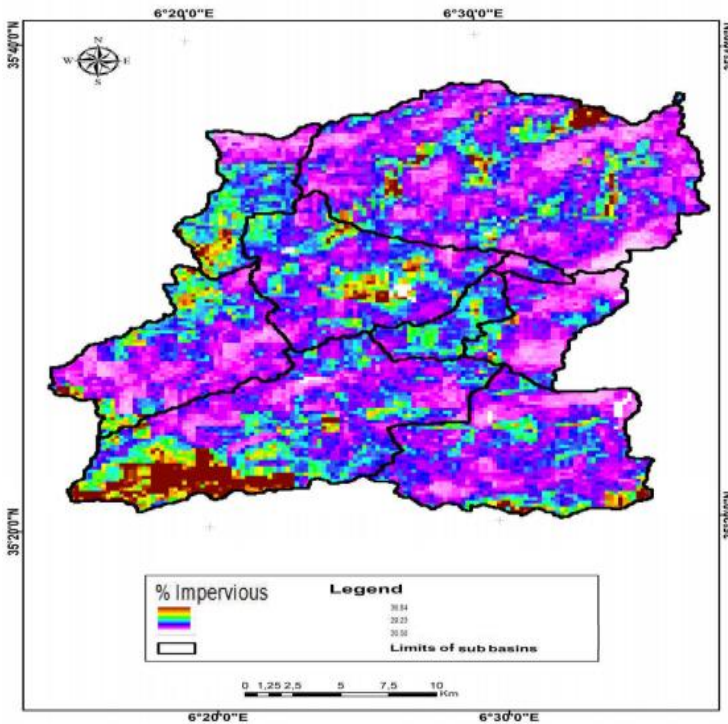


Figure 5: Percentage impervious Map in the Chemora Watershed

Tab. 1. Data used for correlations between NDVI and CN for different soil types NRCS (Arnoldus, 1977)

Cover	NDVI	CN			
		A	B	C	D
Water	0.00	100	100	100	100
Bare soil	0.05	87	90	94	96
Sparse vegetation	0.17	74	83	88	90
Very degraded vegetation	0.29	63	75	83	87
Degraded vegetation	0.38	57	72	81	86
Dense vegetation	0.70	35	56	70	77
Very dense vegetation	0.85	30	44	61	71

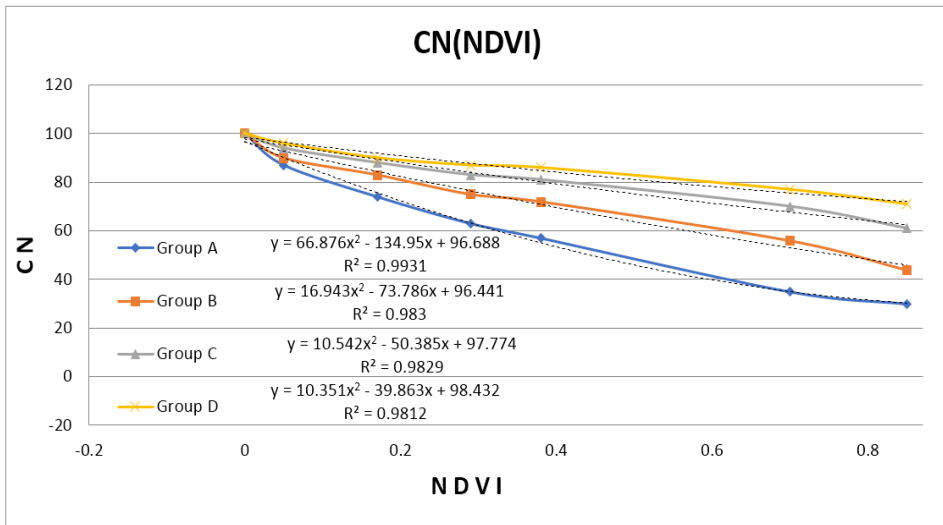


Fig. 6. Correlations between NDVI values and CN values for different types of NRCS soils

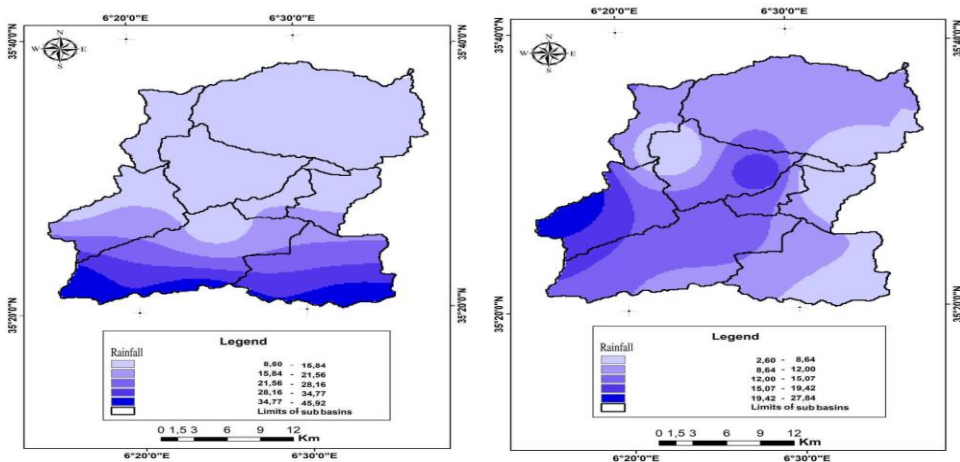


Fig. 7. Rainfall maps of November 15th, 1990 and July 27th, 1991

Calibration and validation of the model

Input data for the HEC-HMS model

Period 1990-1996 was chosen as a basis choice of events for calibration and validation of the model. On the one hand, our choice is due to the unavailability of the satellite images necessary for the preparation of the data before this date, on the other, it is due to the construction of the Koudiet Medaouer dam after this date, which disrupts the hydrological functioning of the basin.

The events recorded during the period September 1990 – August 1991 was chosen the calibration of the model, while those recorded during the periods of September 1995 – August 1996 were chosen for the validation of the model. The dates of the events selected in the first group are as follows: 15 November 1990, 15 March 1991, 10 May 1991, 27 June 1991, and 27 July 1991 and those selected in the second group are: 15 October 1995, 11 January 1996, 08 February 1996 and 15 March 1996.

The input data applied to the HEC-HMS model are:

- The maximum daily rainfall of the sub-basins is estimated from the precipitation maps corresponding to the selected events developed from the data recorded at the rainfall stations mentioned previously (Figure 7).
- For each event, the height of the rain should be associated with each of the four NRCS distributions (1, 1A, 2, and 3).
- The CN values of sub-basins were estimated from the CN maps corresponding to selected events developed from the NDVI maps based on LANDSAT5 satellite images corresponding to the months of the selected events (Figures 8 and 9).
- The values of the percentage of impervious sub-basins estimated from the maps of the percentage of the impervious based on data from www.soilgrids.org (Figure 5).
- The Lag Time values of the sub-basins are calculated by formula 6 (Tables 2 and 3).
- Lag values of rivers are calculated by formula 7 (Table 4).
- Liquid flow values are those recorded at the Chemora hydrometric station.

Tab. 2. The CN and Lag Time values of the sub-basins correspond to the events of the first group calculated by formula 6

S/ BV	November 1990		March 1991		May 1991		June 1991		July 1991	
	CN	T _{lag} (min)	CN	T _{lag} (min)	CN	T _{lag} (min)	CN	T _{lag} (min)	CN	T _{lag} (min)
BV01	90.1	75.1	82.7	98.7	78.2	113.8	81.5	102.6	84.3	93.5
BV02	90.0	91.6	83.4	116.8	78.5	136.7	81.9	122.7	84.8	111.4
BV03	89.6	64.6	80.1	90.5	76.3	101.4	79.1	93.4	81.6	86.3
BV04	90.7	111.9	85.6	136.4	81.3	157.8	86.4	132.3	87.8	125.8
BV05	88.4	185.8	82.9	226.0	79.4	253.1	83.4	222.3	84.6	212.9
BV06	89.3	102.5	83.6	126.5	79.2	145.8	84.5	122.6	85.9	116.7
BV07	89.3	56.2	82.8	71.1	76.3	87.2	82.1	72.8	85.2	65.5
BV08	90.6	17.6	85.1	21.7	81.8	24.2	85.9	21.1	87.3	20.0
BV09	89.9	69.2	84.5	84.8	80.2	97.6	85.3	82.4	86.8	78.0

Tab. 3. The CN and Lag Time values of the sub-basins correspond to the events of the second group calculated by formula 6

S/ BV	October 1995		January 1996		February 1996		March 1996	
	CN	T _{lag} (min)	CN	T _{lag} (min)	CN	T _{lag} (min)	CN	T _{lag} (min)
BV01	60.4	184.4	65.5	161.8	61.2	180.7	56.9	201.4
BV02	62.3	212.8	67.6	185.4	64.0	204.0	60.3	224.1
BV03	55.8	174.8	61.5	151.2	60.6	154.6	59.7	158.1
BV04	61.3	275.1	68.4	228.7	72.4	205.1	76.4	183.0
BV05	51.6	530.8	67.1	357.8	72.7	307.4	78.3	261.2
BV06	56.0	272.1	70.7	185.9	73.6	171.8	76.4	158.3
BV07	60.9	131.9	70.8	101.8	65.7	116.5	60.6	132.7
BV08	51.0	55.7	65.2	38.9	71.5	32.9	77.8	27.4
BV09	45.8	243.8	66.3	144.3	69.3	133.4	72.3	123.0

Tab. 4. River Lag Values calculated by Formula 7

Stream		Length (m)	Slope (m/m)	Lag (min)
SOUDHES_1	Junc_2 - Junc_3	16566	0.0084	217.5
CHEMORA_1	Junc_3 - Excut	19268	0.0065	269.0
ROBOE_0	Junc_1 - Junc_4	11405	0.0075	170.0
ANZA N'ZDIRA	BV_3 - Junc_2	14780	0.0232	134.7
TAGA	BV_2 - Junc_1	25829	0.0228	208.4
IMETSEN	BV_1 - Junc_1	11986	0.0223	116.4
MORRI	BV_5 - Junc_4	6544	0.0151	84.8
TIMGAD (ROBOE_2)	Junc_4 - Junc_3	2005	0.0065	47.3
AIT FDHALA	BV_7 - Junc_2	9347	0.0093	134.5

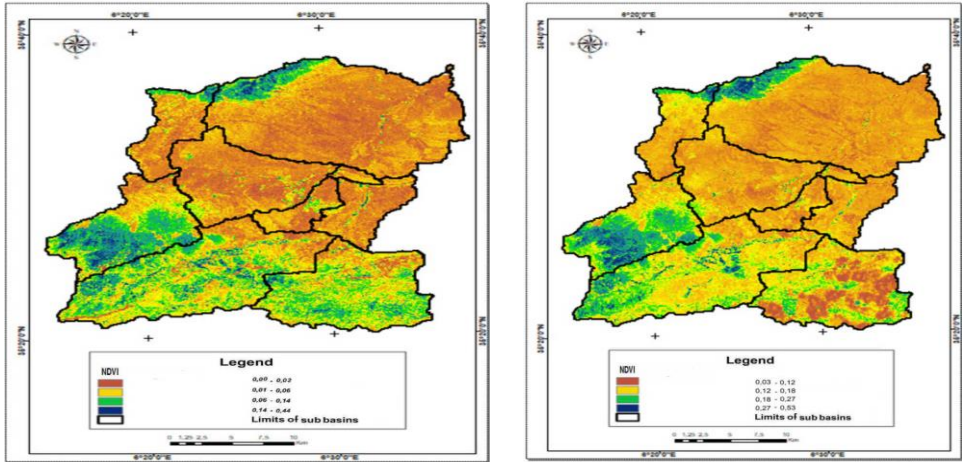


Fig. 8. NDVI Maps November 1990 and July 1991

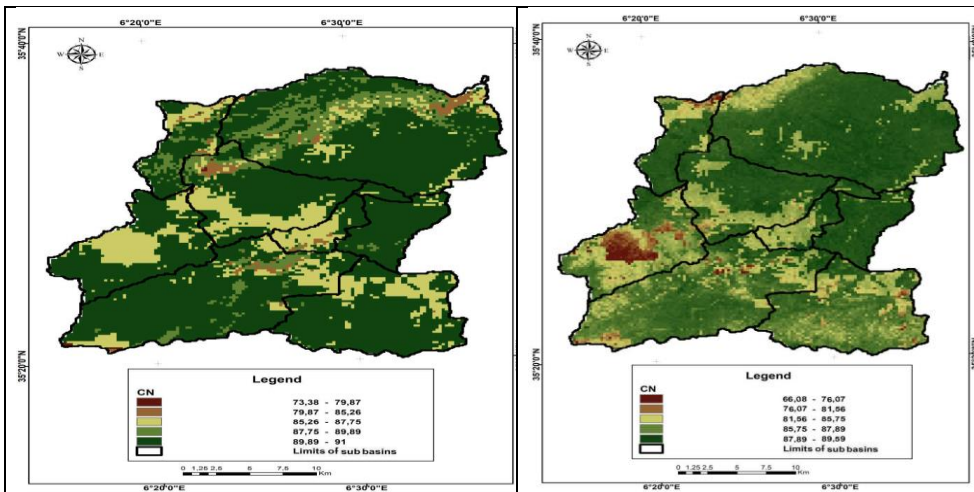


Fig. 9. CN Maps November 1990 and July 1991

Simulation

In order to reach the optimized values of the model parameters, we have prepared all the simulation files for first and second group events, taking into account the four types of NRCS rainfall to analyse the sensitivity of the model successively to the types of precipitations. Therefore, we obtained 20 simulation files.

Comparing the simulated peak flow with the one measured at the Chemora Hydrometric Station, we found that the Type II rainfall were best ranked in the return of hydrograph characteristics.

After the calibration, the validation is performed using the data for second group events by applying the dataset result of the calibration. We reached the following results (Tables 5 and Figure 10).

Tab. 5. Results of the calibration of the hydrological model by the events of the first and the second group

Event	Q_{observed} (m^3/s)	$Q_{\text{simulated}}$ (m^3/s)	Difference %
The first group			
November 15 th , 1990	22.8	16.4	28.1
March 23 th , 1991	183.4	168.8	8.0
May 10 th , 1991	17.9	17.4	2.8
June 27 th , 1991	44.3	41.6	6.1
July 27 th , 1991	5.6	5.1	8.9
The second group			
October 15 th , 1995	150.0	124.2	17.20
January 11 th , 1996	103.6	128.0	11.78
February 07 th , 1996	57.0	66.6	16.84
March 15 th , 1996	147.2	129.3	12.16

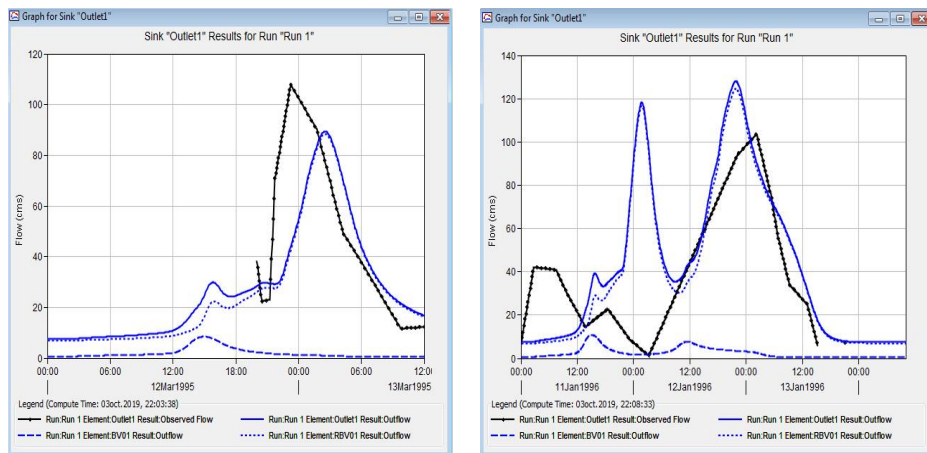


Fig. 10. Hydrographs of simulated and observed flood of October 12th, 1995 and January 11th, 1996

The performance of the model was evaluated by comparing the simulated peak flows with the observed peak flows in terms of relative error (Babel et al., 2004; Najim et al., 2006).

The relative errors calculated during the calibration phase are less than 10%, except in the case of the 15 November 1990 flood, where they are 28.1%, whereas during the model validation phase, they are less than 20%. These errors are considered to be small and the model we have established provides us with reasonably satisfactory results. In conclusion, the application of this model indicates that the formulation used can lead to good results, as long as representative data are available.

Estimation of Flood Flows from rainfall frequency

After calibration and validation of the model, we will evaluate the effect of seasonal changes in vegetation cover on the flood hydrograph resulting from extreme rainfall of different return periods at the site of the Chemora hydrometric station located at the outlet of the basin.

Input data to the HEC-HMS model: The frequency rains of the sub-basins estimated from the maps of the frequency precipitations elaborated starting from the values of these precipitations recorded with the stations rain gauge quoted previously after statistical treatment (Figure 11 and table 6) (Berghout, 2017). The precipitation height should be associated with the NRCS type II distribution.

Tab. 6. Maximum daily frequency precipitation in sub-basins

BVS	frequency rains (10 years)	frequency rains (50 years)	frequency rains (100 years)	frequency rains (1000 years)
BV01	67.3	89.0	98.2	128.5
BV02	64.6	87.7	97.4	129.7
BV03	64.7	87.6	97.3	132.1
BV04	52.2	70.3	78.0	103.2
BV05	56.8	77.2	85.9	114.4
BV06	57.9	78.7	87.5	116.7
BV07	59.8	80.7	89.6	119.5
BV08	54.8	74.5	82.9	110.3
BV09	58.5	79.7	88.7	118.0

The CN values of the sub-basins estimated from the maps of CN corresponding to the different seasons elaborated from the NDVI maps of the year 2011 chosen as an example (Figure 12 and Table 7). The Lag Time values of the sub-basins calculated by the formula 6 (Table 7). Lag values of rivers and impervious percentage values are the same values used in the first part (Table 4). From these maps, we configure separate simulation files for each sub-basin.

Tab. 7. CN and Lag Time values of sub-basins calculated by formula 6

S/ BV	Winter		Spring		Summer		Autumn		Average	
	CN	Tlag	CN	Tlag	CN	Tlag	CN	Tlag	CN	Tlag
BV01	70.2	143.0	64.7	164.9	58.1	195.5	60.5	183.9	63.4	170.9
BV02	72.2	164.1	66.7	190.3	61.4	218.0	57.1	243.1	64.3	202.2
BV03	64.6	139.6	60.6	154.6	60.8	153.7	56.4	171.8	60.6	154.6
BV04	71.7	209.3	68.1	230.5	78.5	172.1	70.5	216.2	72.2	206.4
BV05	60.2	427.8	66.6	362.5	80.2	246.5	71.1	321.2	69.5	335.4
BV06	65.2	215.2	70.1	189.0	78.2	150.2	69.7	191.0	70.8	185.5
BV07	70.8	101.7	70.1	103.7	62.0	128.3	66.0	115.5	67.2	111.9
BV08	59.6	44.8	64.8	39.2	79.8	25.8	63.5	40.6	66.9	37.1
BV09	53.6	199.9	66.1	145.2	74.3	116.3	69.0	134.4	65.7	146.6

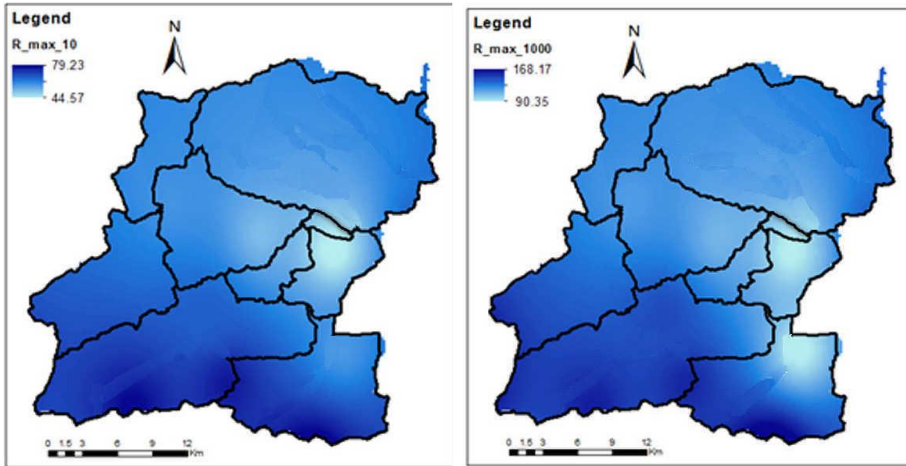


Fig. 11. Frequency rains (10-year) and (1000-year)

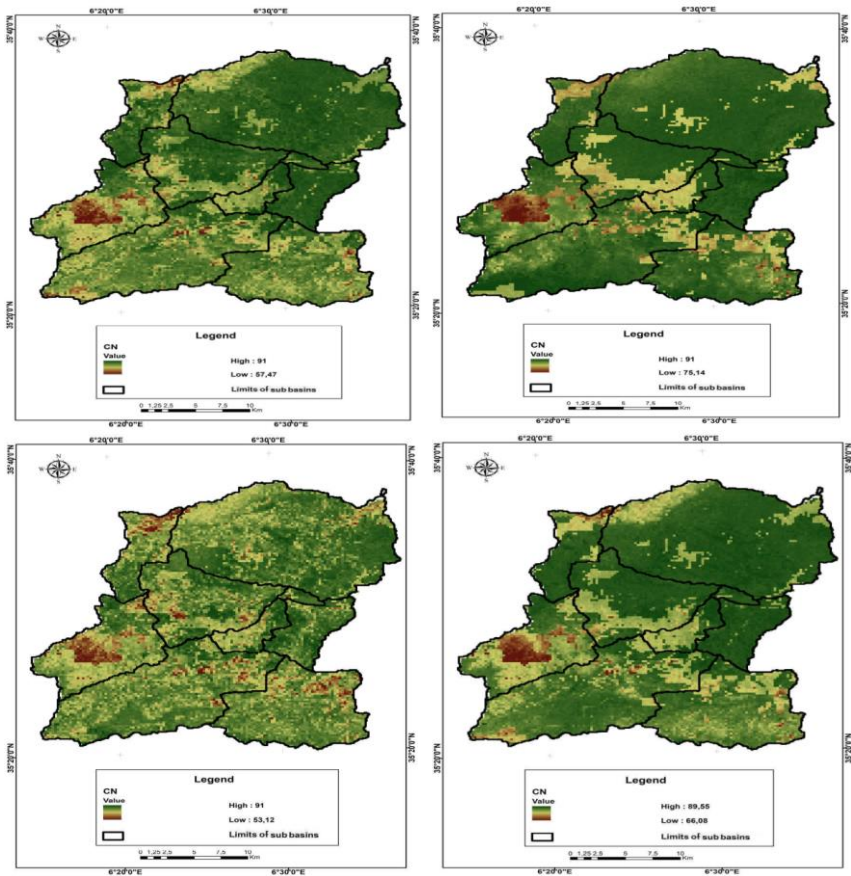


Fig. 12. CN Maps Autumn, Winter, Spring and Summer

Results and discussion

The results summarized in Tables 8, 9, Figures 13, 14, and 15 present the estimated values by the HEC-HMS model in the basin in terms of the peak of the hydrograph and the volume of runoff at the basin outlet, for vegetation cover representing the four seasons and for their annual average (mean NDVI). These data can be used to assess the spatial and temporal variation in peak flows and runoff volume produced by maximum daily rainfall of different frequencies.

Tab. 8. Simulated peak flow and flood volume at the Chemora Station for Quill Rainfall and Four Seasons and for CN average

	T = 10-year	T = 50-year	T = 100-year	T = 1000-year
Winter				
Q _p (m ³ /s)	373.1	614.5	741.6	1172.3
Volume (10 ³ m ³)	15280.2	23977.4	29087.6	45551.5
Spring				
Q _p (m ³ /s)	356.7	561.5	656.1	1011.1
Volume (10 ³ m ³)	<u>17025.6</u>	<u>27220.9</u>	<u>32021.6</u>	<u>49402.2</u>
Summer				
Q _p (m ³ /s)	334.7	524.7	617.3	958.7
Volume (10 ³ m ³)	14528.7	23329.2	28088.4	43311.6
Autumn				
Q _p (m ³ /s)	<u>376.8</u>	<u>631.6</u>	<u>905.4</u>	<u>1408.4</u>
Volume (10 ³ m ³)	14584.0	23640.4	28145.6	43449.1
CN Average				
Q _p (m ³ /s)	368.1	575.7	733.4	1118.1
Volume (10 ³ m ³)	14697.9	23977.4	29010.2	47109.4

The values obtained for the peaks reveal the following. During the autumn season, when there is less vegetation cover, peak flows are at their highest and the relative difference between the peak flow for a given return period and that corresponding to the mean flood of the CN varies between 2.36% for the ten-year flood and 25.96% for the millennial flood. In late spring, when the vegetation cover is dense, peak flows are minimal and the relative difference between the peak flow for a given return period and that corresponding to the average flood of the CN varies between -14.26% for the thousand-year flood and -9.07% for the ten-year flood. In terms of volume, the values obtained show that the maximum water volumes in March (early spring), characterized by moderate vegetation cover, as well as that the minimum water volumes in June (late spring) when the vegetation cover is dense.

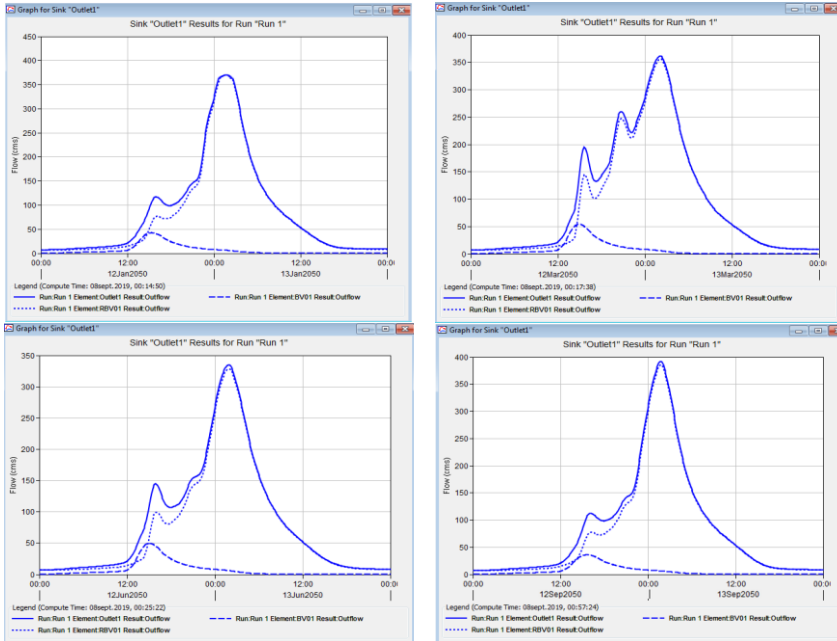


Fig. 13. Simulated 10-year return period flood hydrographs. Month of January (Winter), March (Spring), June (Summer), September (Autumn)

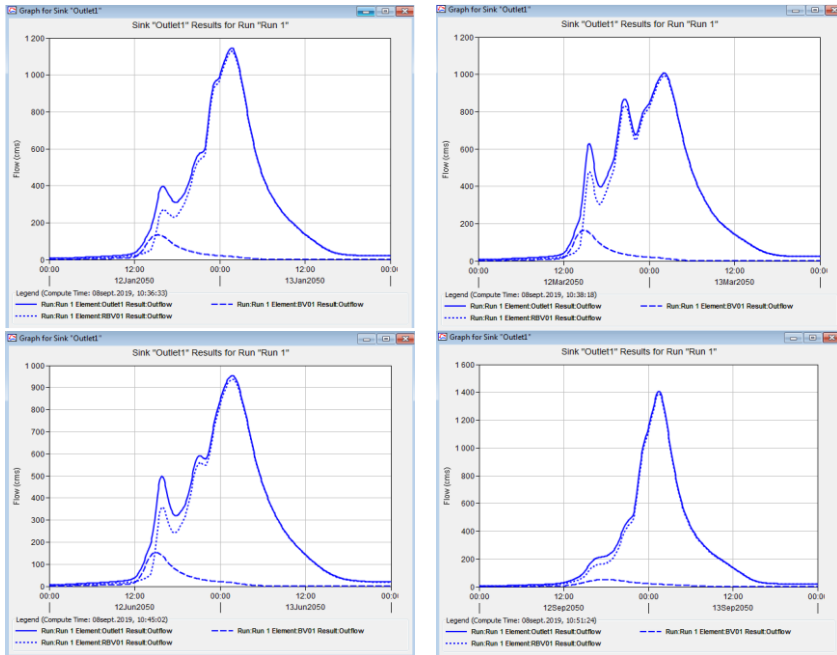


Fig. 14. Simulated 1000-year return period flood hydrographs. Month of January (Winter), March (Spring), June (Summer), September (Autumn)

These results reveal the significant impact of seasonal variations in vegetation cover on the hydrological responses of the catchment to extreme rainfall in terms of peak flow and flood volume.

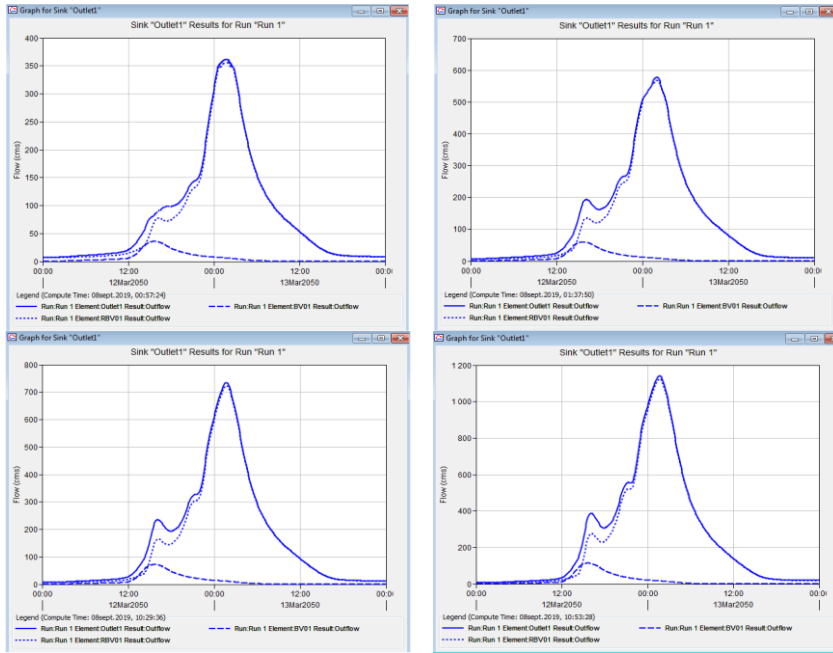


Fig. 15. Simulated 10-year, 50-year, 100-year and 1000-year return period flood hydrographs for CN Average.

Tab. 9. Relative differences between the peak flow, the seasonal flood volume, and those of the flood corresponding to the average CN

	T = 10-year	T = 50-year	T = 100-year	T = 1000-year
Winter				
Relative peak flow difference (%)	1.36	6.74	1.12	4.85
Relative flood volume difference (%)	3.96	0.00	0.27	-3.31
Spring				
Relative peak flow difference (%)	-3.10	-2.47	-10.54	-9.57
Relative flood volume difference (%)	15.84	13.53	10.38	4.87
Summer				
Relative peak flow difference (%)	-9.07	-8.86	-15.83	-14.26
Relative flood volume difference (%)	-1.15	-2.70	-3.18	-8.06
Autumn				
Relative peak flow difference (%)	2.36	9.71	23.45	25.96
Relative flood volume difference (%)	-0.77	-1.41	-2.98	-7.77
Maximum relative differences				
Relative peak flow difference (%)	11.44	18.57	39.28	40.22
Relative flood volume difference (%)	16.99	16.23	13.56	12.93

They confirm the following: 1) The majority of heavy floods causing flooding in the semi-arid regions of North Africa occur in the autumn season (Ali Aït Hssaine, 2014; Noûmène, 2014; Berghout, 2017); 2) The runoff-reducing effect of vegetation cover decreases with high rainfall intensity (Mclvor et al., 1995).

Through this study, we can conclude that in order to assess the characteristics of flood flows in ungauged rivers, necessary for the dimensioning of different structures, in semi-arid regions, where vegetation cover is highly variable, two points need to be studied. First, using statistical tools analyse the autumn flows at the hydrometric stations located near the study area, in order to define the characteristics of these flows, which will then be used to calibrate the hydrological parameters subsequently used for the ungauged rivers. Second, carry out a complete study of the hydrological parameters, in particular the variability of the vegetation cover in the catchment studied, which is essential for hydrological modelling, and admit that the results obtained from an average vegetation cover are far from reality.

Conclusion

With the adequate settings, hydrological modeling by HEC-HMS would be well suited to the semi-arid zone of Chemora. HEC-HMS-SIG would also be useful to estimate frequent flood flows and their spatio-temporal variabilities in semi-arid zones, where the vegetation cover is a strong variable where hydrometric stations are not available, according to rainfall data (maximum frequency daily precipitation).

The values of the extreme flows of the frequency floods estimated by this model corresponds to the vegetation cover in autumn are close to those found by the statistical processing of the measurement data. The study confirms that the most notable peaks result in autumn precipitation where the vegetation cover is weak (where the vegetation cover is weak an increase of 2 % per decennial flood and 26 % for millennial flood compared to flood flows that correspond to median vegetation cover/year) with the lowest water volumes (a decrease between 1% for decennial flood and 8% for millennial flood compared to flood volumes that correspond to the median vegetation cover/year) The weakest peaks result in precipitation in end of spring where the vegetation cover is strong (a decrease of 9 % of decennial flood and 14 % for millennial flood compared to flood flows that correspond to the vegetation cover/year). Water volume being high (an increase of 1% for decennial floods and 8% for millennial floods compared to flood volumes that correspond to the vegetation cover median/year).

These results demonstrate that the effects of changes in vegetation cover during the year on the hydrological responses to precipitation are important in semi-arid zones in Algeria. Consequently, the estimate flood on projects in said zones, where the vegetation cover is a highly probable variable for ungauged basins, using the methods based on daily precipitation are nonetheless insufficient, if we do not take into consideration this variable.

In conclusion, this work is pioneer in semi-arid zones in North Africa. The formulation adopted can lead to good results, as soon as we obtain representative data, it would be possible to extend it to other study sites, and to consider larger scales.

Conflicts of Interest: The authors declare no conflict of interest.

Publisher's Note: Serbian Geographical Society stays neutral with regard to jurisdictional claims in published maps and institutional affiliations.

© 2024 Serbian Geographical Society, Belgrade, Serbia.

This article is an open access article distributed under the terms and conditions of the Creative Commons Attribution-NonCommercial-NoDerivs 3.0 Serbia.

References

- Abdi, I., & Meddi, M. (2020). Comparison of conceptual rainfall – runoff models in semi-arid watersheds of eastern Algeria. *Journal of Flood Risk Management*, 14(1), Article e12672. <https://doi.org/10.1111/jfr3.12672>
- Abdi, I., & Meddi, M. (2020). Study on the applicability of the SCS-CN-based models to simulate floods in the semi-arid watersheds of northern Algeria. *Acta Geophysica*, 69, 217–230. <https://doi.org/10.1007/s11600-020-00511-3>
- Arshad A., Christiaan V., & Fati, A. (2020). Modeling hydrological response to land use/cover change: case study of Chirah Watershed (Soan River), Pakistan. *Arabian Journal of Geosciences*, 13(22), Article 1220. <https://doi.org/10.1007/s12517-020-06177-x>
- Arnoldus, H. M. J. (1977). Methodology used to determine the maximum potential average annual soil loss due to sheet and rill erosion in Morocco. *FAO Soils Bulletin*, 34, 39–51.
- Apollonio, C., Balacco, G., Novelli, A., Tarantino, E., & Piccinni, A. F. (2016). Land use change impact on flooding areas: The case study of Cervaro basin (Italy). *Sustainability*, 8(10), Article 996. <https://doi.org/10.3390/su8100996>
- Babel, M. S., Najim, M. M. M., & Loof, R. (2004). Assessment of agricultural non-point source model for a watershed in tropical environment. *Journal of Environment Engineering*, 130(9), 1032–1041. [https://doi.org/10.1061/\(ASCE\)0733-9372\(2004\)130:9\(1032\)](https://doi.org/10.1061/(ASCE)0733-9372(2004)130:9(1032))
- Benifei, R., Solari, L., Vargas-Luna, A., Geerling, G., & Van Oorschot, M. (2015). Effect of Vegetation on Floods: The Case of the River Magra. *IAHR World Congress 2015*. <https://doi.org/10.13140/RG.2.1.3057.8004>
- Berghout, A., & Meddi, M. (2016). Sediment transport modeling in wadi Chemora during flood flow events. *Journal of Water and Land Development*, 31(10–12), 23–31. <https://doi.org/10.1515/jwld-2016-0033>
- Berghout, A. (2017). *Modeling of solid transport in certain watersheds in North-East Algeria* [Thèse de doctorat, Béjaia University].
- Blondel, J., & Aronson, J. (1999). *Biology and wildlife of the Mediterranean region*. Oxford University Press.
- Cane, C. (1985). Etude d'un modèle pluie - débit type SCS (Soil Conservation Service) Application au bassin versant de l'Aille 'VAR. Office of Geological and Mining Research, Department Marine Geology and Sedimentology.
- Cerdà, A. (1998). The influence of aspect and vegetation on seasonal changes in erosion under rainfall simulation on a clay soil in Spain. *Canadian Journal of Soil Science*, 78(2), 321–330. <https://doi.org/10.4141/S97-060>

- Chang, C. W. (2009). Application of SCS CN Method in HEC-HMS in Shih Men Watershed - Simulation of Rainfall Runoff Hydrologic Model [Doctoral dissertation, Florida State University].
- Combes, F., Hurand, A., & Meunier, M. (1995). La forêt de montagne: un remède aux crues. *Journées de l'hydraulique*, 23(2), 481-486.
- Fehri, N. (2014). L'aggravation du risque d'inondation en Tunisie: éléments de réflexion. *Géographie Physique et environnement*, 8, 149-175. <https://doi.org/10.4000/physio-geo.3953>
- Hu, S., & Shrestha, P. (2020). Examine the impact of land use and land cover changes on peak discharges of a watershed in the mid-western United States using the HEC-HMS model. *Papers in Applied Geography*, 6(2), 101-118. <https://doi.org/10.1080/23754931.2020.1732447>
- Hssaine, A. A. (2014). Éléments sur l'hydrologie de la partie atlasique de l'oued Guir (Maroc sud-oriental) et sur l'inondation catastrophique du 10 octobre 2008. *Géographie Physique et environnement*, 8, 337-354. <https://doi.org/10.4000/physio-geo.4292>
- Ibrahim-Bathis, K., & Ahmed, S. A. (2016). Rainfall-runoff modelling of Doddahalla watershed—an application of HEC-HMS and SCN-CN in ungauged agricultural watershed. *Arabian Journal of Geosciences*, 9, Article 170. <https://doi.org/10.1007/s12517-015-2228-2>
- Ioannidou, V. G., & Arthur, S. (2020). Experimental results of the hydrological performance of a permeable pavement laboratory rig. *Journal of Water Supply: Research and Technology—Aqua*, 69(3), 210-223. <https://doi.org/10.2166/aqua.2020.118>
- Johnson, F., Xuereb, K., Jeremiah, E., & Green, J. (2012). Regionalisation of rainfall statistics for the IFD revision project. *34th Hydrology and Water Resources Symposium*.
- Koneti, S., Sunkara, S. L., & Roy, P. S. (2018). Hydrological Modeling with Respect to Impact of Land-Use and Land-Cover Change on the Runoff Dynamics in Godavari River Basin Using the HEC-HMS Model. *International Journal of Geo-Information*, 7(6), Article 206. <https://doi.org/10.3390/ijgi7060206>
- Lavabre, J., Andreassian, V., & Laroussinie, O. (2000). Eaux et forêts: la forêt, un outil de gestion des eaux? *La Houille Blanche*, 88(3), 72-77. <https://doi.org/10.1051/lhb/2002047>
- Li, W., & Sankarasubramanian, A. (2012). Reducing hydrologic model uncertainty in monthly stream flow predictions using multimodel combination. *Water Resources Research*, 48(12), 1-17. <https://doi.org/10.1029/2011WR011380>
- Meddi, M., Toumi, S., & Assani, A. A. (2017). Application of the L-moments approach to the analysis of regional flood frequency in Northern Algeria. *International Journal of Hydrology Science and Technology*, 7(1), 77 - 102. <https://doi.org/10.1504/IJHST.2017.080959>
- McIvor, J. G., Williams, J., & Gardener, C. J. (1995). Pasture management influences runoff and soil movement in the semi-arids tropics. *Australian Journal of Experimental Agriculture*, 35(1), 55-65.
- Mendas, M., Errih, M., & Bouchenak, F. (2008). Hydrologic model combined with a GIS for estimating hydrologic balance at watershed scale: application to the Mac-ta watershed (north-western Algeria). *Journal of Water Supply: Research and Technology—Aqua*, 57(5), Article 360. <https://doi.org/10.2166/aqua.2008.039>

- Nazari-Sharabian, M., Taheriyoun, M., & Karakouzian, M. (2020). Sensitivity analysis of the DEM resolution and effective parameters of runoff yield in the SWAT model: a case study. *Journal of Water Supply: Research and Technology—Aqua*, 69(1), 39–54. <https://doi.org/10.2166/aqua.2019.044>
- National Hydric Resources Agency. (2005). *Annuaire des précipitations de l'Algérie (Rainfall directory of Algeria)*. National Hydric Resources Agency.
- Razavi, T., & Coulibaly, P. (2012). Stream flow prediction in ungauged basins: review of regionalization methods. *Journal of Hydrologic Engineering*, 8(8), 958–975. [https://doi.org/10.1061/\(ASCE\)HE.1943-5584.0000690](https://doi.org/10.1061/(ASCE)HE.1943-5584.0000690)
- Richard, D., & Mathys, N. (1999). Historique, contexte technique et scientifique des BVRE de Draix. Caractéristiques, données disponibles et principaux résultats acquis au cours de dix ans de suivi. *Proceedings of the conference “The experimental water sheds of Draix, laboratory for the study of mountain erosion”*.
- Sarhadi, A., & Modarres, R. (2011). Flood seasonality-based regionalization methods: a data based comparison. *Hydrological Process*, 25(23), 3613–3624. <https://doi.org/10.1002/hyp.8088>
- Scharffenberg, W. (2016). *Hydrological Modeling System HEC-HMS. User's Manual*. Hydrologic Engineering Center.
- Shrestha, B. B. (2019). Approach for Analysis of Land-Cover Changes and Their Impact on Flooding Regime. *Quaternary*, 2(3), Article 27. <https://doi.org/10.3390/quat2030027>
- United States Agency for International Development. (2010). *Hydrology National Engineering Handbook*. United States Agency for International Development
- United States Army Corps of Engineers. (2013). *Hydrologic Modeling System HEC-HMS Version 4.0*. United States Army Corps of Engineers.
- Velázquez, J. A., Antil, F., & Perrin, C. (2010). Performance and reliability of multi-model hydrological ensemble simulations based on seventeen lumped models and a thousand catchments. *Hydrology and Earth System Sciences*, 14(11), 2303–2317. <https://doi.org/10.5194/hess-14-2303-2010>
- Yahi, A., & Rezoug, B. (2019). *Modélisation Hydrologique (pluie - débit) pour plusieurs Scénarios d'occupation du sol cas du Bassin Versant de Chemora – Batna* [Master's thesis, Msila University].
- Zheng, Y., Li, J., Dong, L., Rong, Y., Kang, A., & Feng, P. (2020). Estimation of Initial Abstraction for Hydrological Modeling Based on Global Land Data Assimilation System—Simulated Data sets. *Journal of Hydrometeorology*, 21(5), 1051–1072. <https://doi.org/10.1175/JHM-D-19-0202.1>